JOURNAL OF MATERIALS SCIENCE 19 (1984) 1680–1691

Analysis of the effect of embedded fibre length on fibre debonding and pull-out from an elastic matrix

Part 2 *Application to a steel fibre–cementitious matrix composite system*

R. J. GRAY
Department of Civil Engineering, The University of British Columbia, Vancouver, British Columbia, V6T 1W5, Canada.

Experimental results obtained from single fibre pull-out tests on specimens with different fibre embedment lengths, consisting of a brass-coated steel wire as fibre and a cementitious mortar as matrix, are analysed using the appropriate theories reviewed in the first part of this paper. The analyses indicate that both adhesional bonding and frictional resistance to slipping along the portion of the interface over which the adhesional bond has failed contribute significantly to the total resistance to completion of fibre debonding and initiation of fibre pull-out in these specimens. Estimated values of the adhesional (maximum) interfacial bond shear strength and the frictional resistance to slipping obtained from the apparent variation of maximum pull-out load with embedded fibre length are compared and found, for theories which are similar, to be generally in agreement.

1. Introduction

Several of the theories developed to explain the interfacial debonding and pull-out processes in composites composed of ductile fibres in a brittle or elastic matrix, and to enable estimation of the parameters representing the debonding and/or pull-out resistance are reviewed in the first part of this paper [1]. The applicability of these theories to pull-out test results for steel fibres in a cementitious matrix is examined in this second part.

Most of the theories reviewed have been applied to experimental test data only to a limited extent, even by the proponents themselves, but some have been used previously for composites with cement-based matrices. For example, Beaumont and Aleszka [2] have used the methods proposed by both Greszczuk [3] and Takaku and Arridge [4] to analyse the results of single-fibre pull-out tests on specimens consisting of a brass-coated steel wire as fibre and either a plain or a polymer impregnated mortar as matrix. A nonlinear relationship between the stress in the fibre at both debonding and initial pull-out and the embedded fibre length was observed. For each type of matrix, the values of the average interfacial bond strength, $\tau_{ib,av}$,* were calculated from the measured debonding loads, and an estimate of the maximum bond strength, $\tau_{ib,max}$, was obtained using the graphical method proposed by Greszczuk [3]: this strength was 9.0 MPa for the plain and 19.5 MPa for the polymer impregnated mortar matrices. Analysis of the initial pull-out loads using the method proposed by Takaku and Arridge [4] resulted in estimated values of 19.2 MPa and 32.6 MPa for the normal compressive stress, $\sigma_{i,n}$, exerted by the plain and the polymer impregnated mortar matrices, respectively, on the fibre across the interface, and of 0.6 for the interfacial coefficient of

*The same notation is used as in Part 1 [1].

0022–2461/84 $03.00 + .12

friction, μ, between both types of matrix and the fibre.

Bowling and Groves [5] employed their own theoretical model to evaluate single-fibre pull-out test results obtained using specimens consisting of nickel wire embedded in a cement paste matrix. At sufficiently long fibre embedment lengths, a debonding plateau was observed in the pull-out stress–fibre displacement diagram at a stress somewhat in excess of the yield stress of the fibre. However, variations in the fibre stress during debonding and in the observed debonding plateau lengths were too large to give useful results or to indicate the form of the relationship between fibre debonding stress and embedded fibre length.

Pull-out test results for E-glass fibre strands embedded in a cement paste matrix have been analysed by Bartos [6] using his own graphical technique [7]. Three failure modes were observed in these specimens: complete fibre/matrix debonding followed by fibre pull-out; fibre tensile failure; and partial fibre/matrix debonding followed by fibre tensile failure. However, the absence of a suitable method for determining the extent of partial debonding preceding fibre failure limited the analysis to the results of tests in which complete fibre debonding and pull-out occurred. Elastic and frictional shear flow resistance values were obtained from the pull-out load–fibre displacement curve for each specimen, and were treated statistically to obtain mean values, and corresponding measures of variability, for the fibre–matrix combination examined.

Laws [8] has re-examined data obtained by DeVekey and Majumdar [9], who used pull-out specimens consisting of various types of fibres and cementitious matrices, with a very small fibre embedment length (1.0 mm). Pull-out load–fibre displacement curves for certain combinations of steel wire fibre, cement paste matrix, and specimen curing conditions showed either a discontinuity (peak) or a change in slope before the maximum load was reached, suggesting a progressive debonding process. The point of discontinuity or change in slope was assumed to mark the beginning of debonding and was used, together with the maximum load and the "constant" frictional load during pull-out of the fibre, to calculate appropriate interfacial bond strength values. For specimens containing "bright" high tensile steel wire fibre, and cured in water for 28 days, these values are: average bond strength ($\tau_{ib,av}$), 5.5 MPa; maximum bond strength ($\tau_{ib,max}$), 7.4 MPa; "frictional bond" strength ($\tau_{ib,f}$), 4.9 MPa; and "cohesive bond" strength, 2.5 MPa.

To date, however, no single set of experimental pull-out test data has been analysed using two or more of the theories reviewed. Examination of such a set of data is needed to permit comparison of these theories, and to assess the merits and applicability of each in explaining debonding and pull-out behaviour and/or in providing numerical estimates of the various interfacial bond shear "strength" values. Analyses of experimental data obtained by the author for this purpose [10], using several of these theories, are therefore presented in this paper.

2. Experimental method

Single-fibre pull-out tests were performed with a steel wire as fibre and a cementitious mortar as matrix, using a test specimen and configuration described previously [11]. The steel wire was brass-coated, had a diameter of 0.38 mm and a tensile strength of 2550 MPa, and was cleaned with trichlorethane and a water-based alkaline surface cleaner. The cementitious mortar matrix consisted of normal Portland cement and a natural fine aggregate, with mix proportions sand:cement:water = 3.0:1.0:0.5. The specimens were cast horizontally, with the embedded fibre perpendicular to the direction of casting and compaction. For each of the five fibre embedment lengths examined, eight specimens were prepared and tested after curing in water for 28 days.

3. Experimental results

The maximum fibre pull-out or fibre fracture load for each of the specimens is plotted against the corresponding fibre embedment length in Fig. 1. The pull-out load data and the debonding and pull-out resistance values calculated therefrom, required in the various analyses, are summarized in Table I.

All of the specimens with embedded fibre lengths up to an including 100 mm failed by fibre debonding and pull-out. Two distinctly different forms of failure, identified as "progressive" and "catastrophic" on the basis of the debonding process indicated by the variation of the pull-out load during the test, were observed. Typical load against time patterns for these failure modes, obtained with a strip chart recorder, are reproduced in Fig. 2: the progressive failure pattern

TABLE I Summary of pull-out load data and debonding and pull-out resistance values

Embedded fibre length, l_e (mm)		Maximum pull-out (debonding)/failure load, $P_{f,max}$ (N)	Average interfacial bond strength, $\tau_{ib,av}$ (MPa)	Fibre debonding/failure stress $\sigma_{f,max}$ (MPa)	Apparent pull-out load $(P_{f,max}-P_{f,d})^*$ (N)	Fibre pull-out stress $\sigma_{f,po}$ (MPa)	Residual fibre load $P_{f,r}{}^*$ (N)	Frictional shear flow resistance $P_{f,r}/l_e$ (N mm^{-1})
25	mean	88	2.9	780	35	310	44	1.8
	standard deviation	27			20		23	
	coefficient of variation (%)	31			58		52	
50	mean	130	2.1	1150	65	570	75	1.5
	standard deviation	57			37		39	
	coefficient of variation (%)	44			56		53	
75	mean	167	1.8	1470	76	670	192	1.4
	standard deviation	39			21		20	
	coefficient of variation (%)	23			27		20	
100	mean	177	1.5	1560	81	710	107	1.1
	standard deviation	31			37		39	
	coefficient of variation (%)	17			46		37	
125	mean†	265		2340				

*See Fig. 7a [1].

†Based on 5 specimens which failed by fibre fracture rather than pull-out.

Figure 1 Pull-out test results.

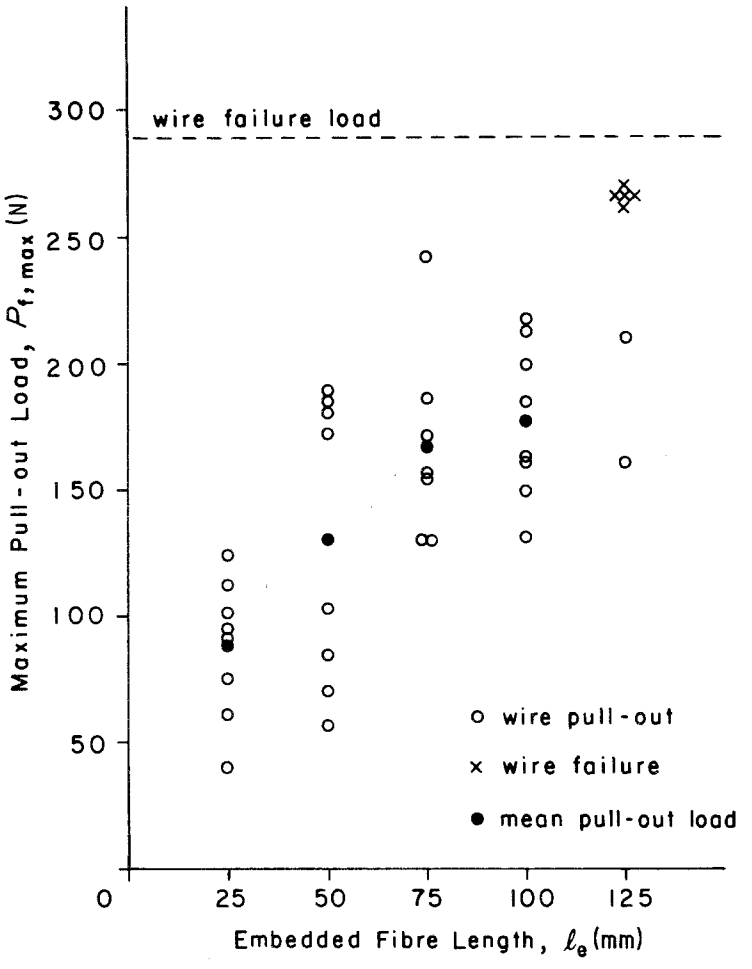

clearly shows a change in slope before the maximum load point is reached.

Most of the specimens with a fibre embedment length of 125 mm failed by fibre fracture rather than pull-out, the fractures occurring at slightly lower loads than the expected failure load calculated from the measured tensile strength of the wire. The majority of these fractures occurred in the wire grip, and the remainder at the point where the wire entered the matrix block.

4. Analysis of experimental results

The results reported in Fig. 1 show considerable scatter, as is commonly observed in pull-out test data for cementitious matrix specimens [12], and consequently the relationship between maximum pull-out load and fibre embedment length represented by these results is open to several interpretations. The maximum pull-out load does not, however, appear to be directly proportional to embedded fibre length.

The mean values, plus and minus one standard deviation, of the calculated average interfacial bond shear strength, $\tau_{ib,av}$, for the specimens which failed by fibre pull-out, reported in Table I, are plotted against fibre embedment length, l_e, in Fig. 3. According to Greszczuk [3], an estimated value of the maximum interfacial bond shear strength, $\tau_{ib,max}$, can be obtained by fitting a smooth curve conforming to the theoretical relationship between $\tau_{ib,av}$ and l_e, i.e.

$$\tau_{ib,av} = \frac{\tau_{ib,max}}{\alpha_1 l_e \coth \alpha_1 l_e} \quad (1)$$

to such data and extrapolating it back to an embedded fibre length of zero. The solid line shown in Fig. 3 represents a trial and error fit of the above equation to the experimental data, assuming that: (a) the value of the elastic constant α_1 is 0.024, and, (b) the broken line extrapolation gives a value of 3.3 MPa for $\tau_{ib,max}$. As this analytical method does not take into account the

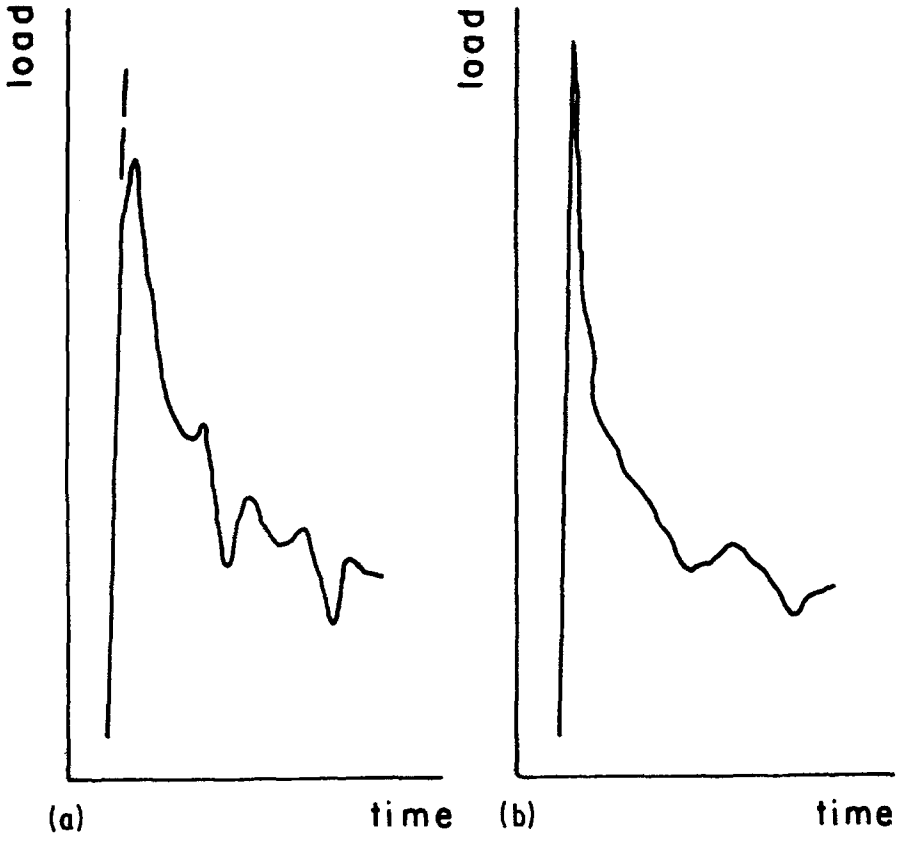

Figure 2 Typical pull-out load against time patterns. (a) Progressive failure and (b) catastrophic failure.

test results for the 125 mm specimens which failed by fibre fracture rather than pull-out, the fit of this curve and hence the derived value for $\tau_{ib,max}$ are sufficiently accurate for the purpose of this examination.

The mean values of the maximum pull-out load, $P_{f,max}$, plus and minus one standard deviation, are plotted against embedded fibre length in Fig. 4. These data indicate that the relationship between $P_{f,max}$ and l_e is linear beyond a certain embedded fibre length. Consequently, according to Lawrence [13], frictional resistance forces are involved in the load transfer process and hence the "frictional" interfacial bond shear strength, $\tau_{ib,f}$, is not equal to zero, i.e. $\tau_{ib,max}/\tau_{ib,f}$ is less than infinity. Values for the embedded fibre length at which the slope of the $P_{f,max} - l_e$ curve becomes constant, $l_{e,min}$, and the slope, $\alpha_2\Delta$, can be determined and substituted in the equation given by Lawrence, namely,

$$\tau_{ib,max} = \frac{\alpha_2\Delta}{\pi d_f}\cosh^2\alpha_2 l_{e,min} \qquad (2)$$

to obtain a value for $\tau_{ib,max}$.

From the data given in Table II, $\alpha_2 = 1.10\,mm^{-1}$, and from the least squares linear

TABLE II Properties and dimensions of the fibre and matrix

Property/Dimension	Fibre	Matrix	
Modulus of elasticity	$E_f = 207$ GPa	$E_m = 30.4$ GPa	Anson and Newman [18]
Poisson's ratio	$\nu_f = 0.27$	$\nu_m = 0.17$	
Shear modulus*		$G_m = 18.3$ GPa	
Radius	$r_f = 0.19$ mm	$r_m = 12.7$ mm	
Cross-sectional area	$A_f = 0.11$ mm^2	$A_m = 507$ mm^2	

*$G_m = \dfrac{E_m}{2(1-\nu_m)}$.

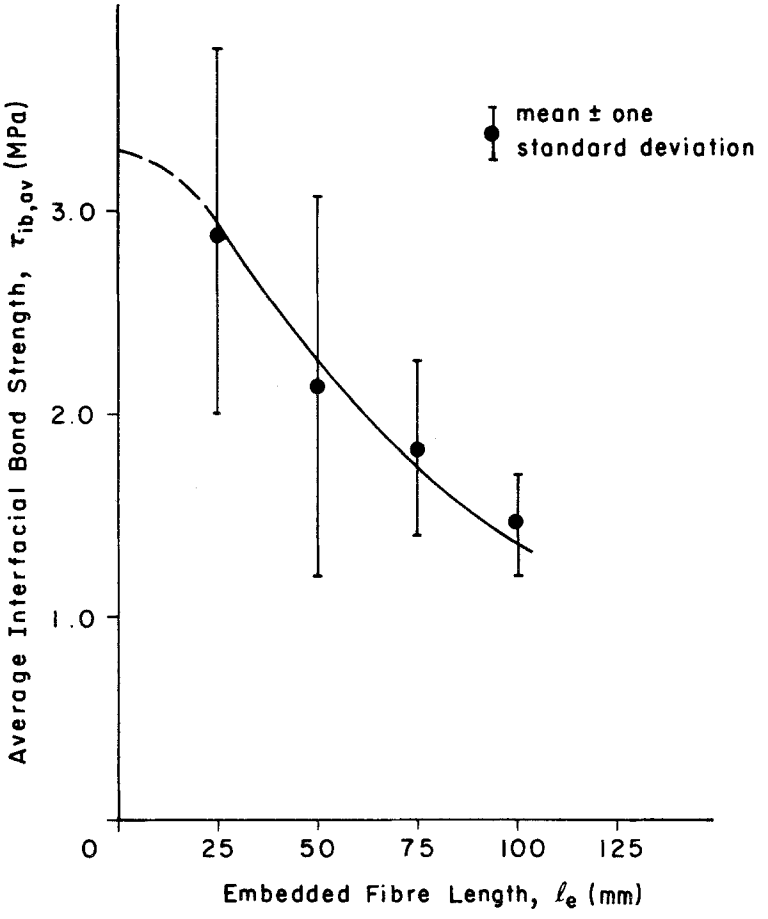

Figure 3 Variation of average interfacial bond strength with embedded fibre length.

regression between $P_{f,max}$ and l_e, shown by the line DAB in Fig. 4, $\alpha_2\Delta = 1.60\,N\,mm^{-1}$. As the curve representing the variation of $P_{f,max}$ with l_e for $l_e \leqslant l_{e,min}$, namely,

$$P_{f,max} = \frac{\tau_{ib,max}\pi d_f}{\alpha_2}\tanh\alpha_2 l_e \qquad (3)$$

shown by the line OAC in Fig. 4, is tangent to DAB at $l_e = l_{e,min}$, i.e. at point A, a trial and error method can be used to solve for $l_{e,min}$, and hence $\tau_{ib,max}$. The results are $l_{e,min} = 2.2\,mm$ and $\tau_{ib,max} = 45.0\,MPa$. A value for $\tau_{ib,f}$ can be obtained by substitution in

$$\tau_{ib,f} = \frac{\alpha_2\Delta}{\pi d_f} \qquad (4)$$

which gives $\tau_{ib,f} = 1.3\,MPa$, and therefore $\tau_{ib,max}/\tau_{ib,f} \sim 35$.

The theoretical variation of $P_{f,max}$ with l_e for small values of l_e, according to Lawrence [13], is shown in Fig. 5.

The test results are presented in a form suitable for analysis using the method proposed by Takaku and Arridge [4] in Fig. 6. The "normalized" curve shown in this figure represents the relationship between $\tanh l_e$ and l_e, whilst the "experimental" curve represents the observed relationship between the stress in the fibre at the maximum pull-out load, $\sigma_{f,max}$, and l_e. The experimental values of $\sigma_{f,max}$ are reported in Table I. It should be noted that: (a) the experimental curve has been drawn through the test results to be of the same shape as the normalized curve and, as near as possible, parallel to it; and, (b) the results for the specimens with a 125 mm fibre embedment length have not been included in the analysis as fibre failure rather than pull-out occurred.

The "shift distances" shown in Fig. 6, from which values for $\tau_{ib,max}$ and an elastic constant α_3 are determined, are taken as the ratios of equivalent points on the normalized and experimental curves. The calculated values for these two parameters are $\tau_{ib,max} = 3.1\,MPa$ and $\alpha_3 = 0.02\,mm^{-1}$.

The $\sigma_{f,max}$ values are also plotted against the corresponding embedded fibre lengths in Fig. 7.

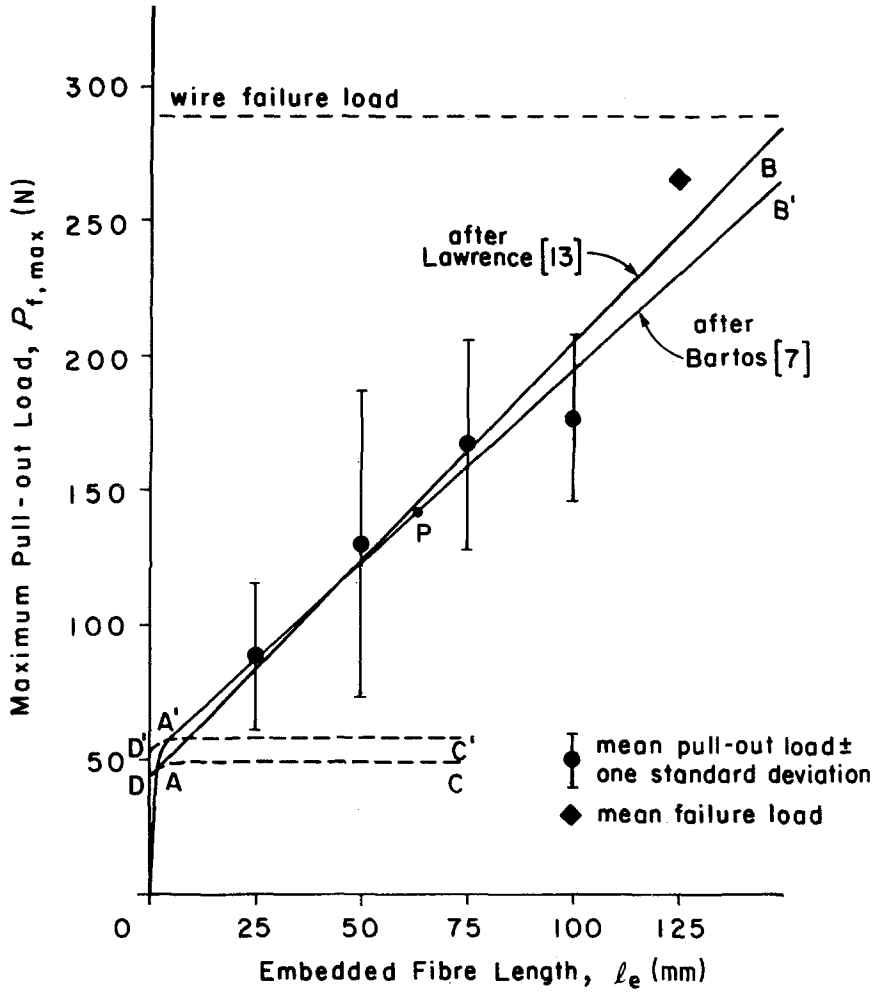

Figure 4 Variation of maximum pull-out load with embedded fibre length.

The solid line shown in this figure represents the theoretical relationship between $\sigma_{f,max}$ and l_e on the basis of the equation proposed by Takaku and Arridge, i.e.

$$\sigma_{f,max} = \frac{2\tau_{ib,max}}{r_f \alpha_3} \tanh \alpha_3 l_e \qquad (5)$$

and the calculated values of $\tau_{ib,max}$ and α_3 given above. This relationship obviously fits the results for the specimens which failed by fibre debonding and pull-out quite well, but does not account for the specimens which failed by fibre fracture. It should be recalled that Takaku and Arridge also do not consider the contribution of frictional forces at the interface after the initial adhesional/elastic bond has broken in assessing the total resistance to debonding.

The value of the constant α_3 obtained from the analysis of the experimental data, 0.02 mm^{-1}, differs significantly from that obtained by substituting the requisite data from Table II into the appropriate theoretical equation (see Part 1), 1.2 mm^{-1}. Takaku and Arridge suggest that a comparison of these two values gives an indication of the proportion of the fibre/matrix interfacial bond area over which adhesional bonding is "perfect" before commencement of the debonding process.

Experimental values of the stress in the fibre at the initiation of pull-out, $\sigma_{f,po}$, as defined by Takaku and Arridge, are also reported in Table I and plotted against the corresponding embedded length in Fig. 7. These results apparently fit reasonably well the theoretical relationship between $\sigma_{f,po}$ and l_e proposed by these authors, i.e.

$$\sigma_{f,po} = C_1[1 - \exp(-C_2 l_e)] \qquad (6)$$

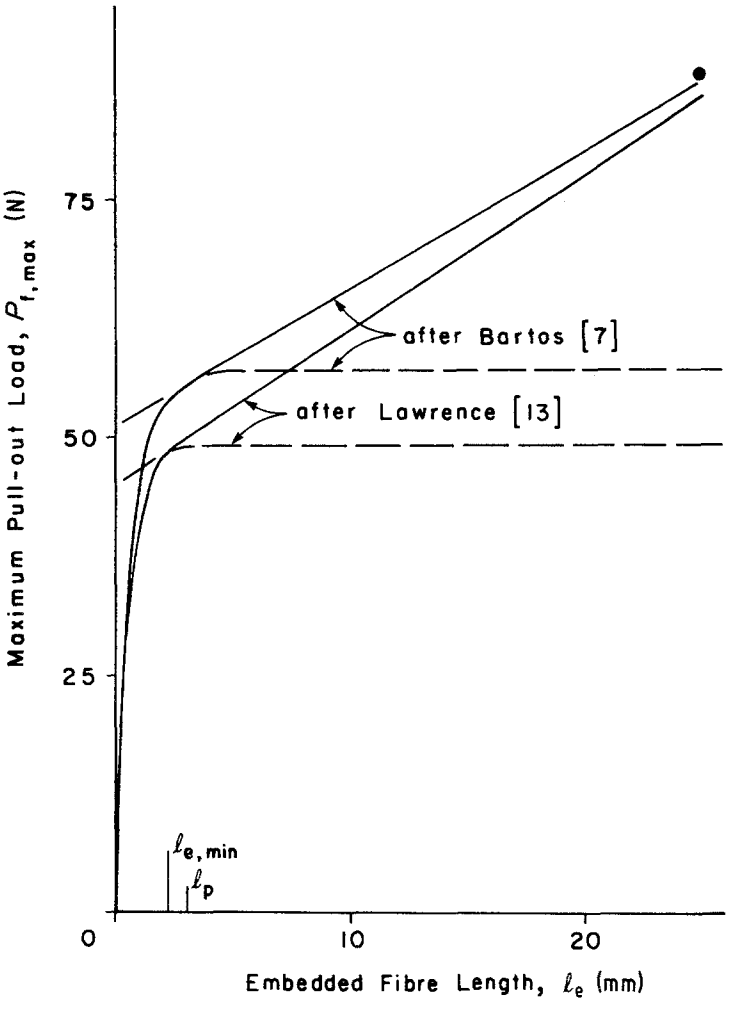

Figure 5 Theoretical variation of maximum pull-out load with embedded fibre length at short embedment lengths.

A graphical method has been used to determine values for C_1, a function of the normal compressive stress exerted by the matrix on the fibre across the interface, $\sigma_{i,n}$, and C_2, a function of the coefficient of friction between the fibre and the matrix at the interface, μ, from the experimental data. Substitution of these values, i.e. $C_1 = 725\,\text{MPa}$ and $C_2 = 0.032\,\text{mm}^{-1}$, in the above equation gives the broken line shown in Fig. 7, and in the appropriate theoretical formulae (see Part 1) gives $\sigma_{i,n} = 24.6\,\text{MPa}$ and $\mu = 0.09$.

Pinchin and Tabor [14, 15] also express the dependence of $\sigma_{f,po}$ on l_e in the form of Equation 6, but propose that C_1 is a function of the fibre/matrix misfit, λ, which is the difference between the radius of the fibre and the radius of the hole in the matrix in the absence of the fibre. The value of C_1 obtained from the experimental results gives an estimated value of $0.18\,\mu\text{m}$ for λ.

The test results obtained in this investigation can also be analysed using the graphical technique proposed by Bartos [7]. Rather than assessing pull-out load–fibre displacement curves for each specimen separately [6], however, the average pull-out load values reported in Table I, and plotted against the corresponding fibre embedment length in Fig. 4, are used in the analysis.

The average of the mean maximum pull-out load values and the corresponding average embedded fibre length, for only those specimens which failed by fibre debonding and pull-out, is represented by point P in Fig. 4. The slope of the straight line D′A′B′ passing through P is equal to the frictional shear flow resistance to slipping at the interface, $q_{ib,f}$, and is taken as the average of the $P_{f,r}/l_e$ values reported in Table I, i.e. $q_{ib,f} = 1.45\,\text{N mm}^{-1}$. The curve representing the variation of $P_{f,max}$ with l_e for $l_e \leqslant l_p$, where l_p is the maximum embedded fibre length at which complete debonding occurs instantaneously, is given by

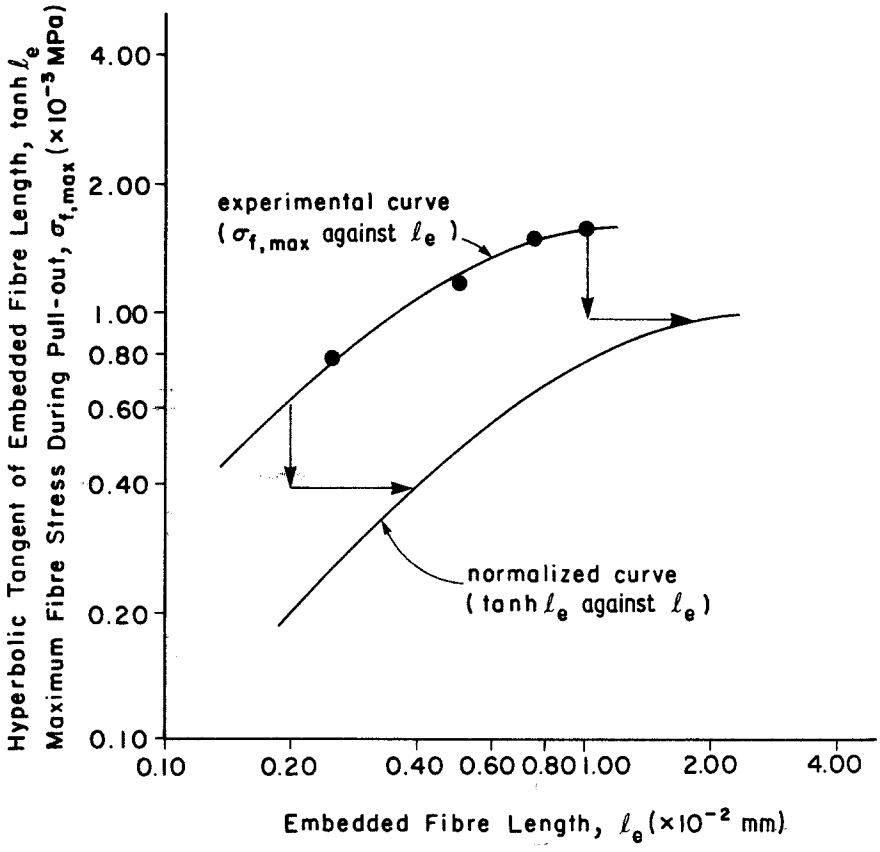

Figure 6 Variation of maximum fibre stress during pull-out with embedded fibre length.

$$P_{f,max} = \frac{q_{ib,max}}{\alpha_4} \tanh \alpha_4 l_e \qquad (7)$$

Since this curve, shown by the line OA'C', is tangent to D'A'B' at $l_e = l_p$, i.e. at point A', a trial and error method can also be used to solve for l_p and hence $q_{ib,max}$, the elastic shear flow resistance to fibre/matrix interfacial debonding. The results are $l_p = 3.0\,\text{mm}$ and $q_{ib,max} = 45.8\,\text{N mm}^{-1}$, where the elastic constant $\alpha_4 = 0.80\,\text{mm}^{-1}$ from the data given in Table II. As the perimeter of the steel wire fibre used in these tests is easily determined, the interfacial bond strength values obtained from these shear flow resistance values are $\tau_{ib,f} = 1.2\,\text{MPa}$ and $\tau_{ib,max} = 38.4\,\text{MPa}$.

The theoretical variation of $P_{f,max}$ with l_e for small values of l_e, according to Bartos [7], is also shown more clearly in Fig. 5.

Unfortunately, the pull-out load–time curves for only a very small number of the test specimens exhibited the "progressive" failure pattern shown in Fig. 2a. These curves have a definite change in slope, taken as the beginning of a progressive debonding process, before the maximum load point is reached, and hence correspond to the progressive pull-out load–fibre displacement curve described by Laws [8] in her extension of Lawrence's theory. For these few specimens, "average" values of the maximum, average, and "frictional" interfacial bond shear strengths, as calculated from the pull-out load values at appropriate points on their curves using Laws' equations, are 94.7, 1.8 and 1.2 MPa, respectively. The relationship of these values to each other generally agrees with that predicted theoretically by Laws (see Fig. 3 [8]).

5. Discussion

Values of the maximum shear strength of the fibre/matrix interfacial bond, $\tau_{ib,max}$, and the frictional resistance to slipping at the interface after debonding has occurred, $\tau_{ib,f}$, obtained through application of the relevant theoretical analyses reviewed in Part 1 of this paper to a set of experimental pull-out test results obtained by the author are summarized in Table III.

The two analyses which do not take frictional

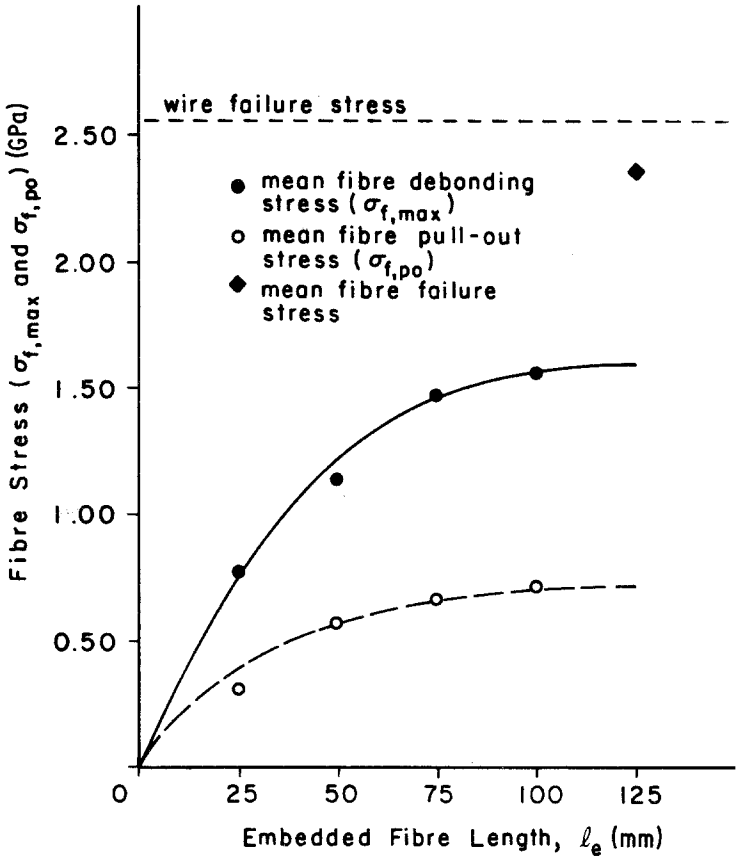

Figure 7 Variation of fibre stress with embedded fibre length.

resistance to slipping over a debonded portion of the interface into consideration in assessing the total resistance to complete fibre debonding and initiation of pull-out, i.e. those proposed by Greszczuk [3] and Takaku and Arridge [4], give about the same value for the maximum interfacial bond shear strength. This value is, however, approximately one order of magnitude smaller than that obtained using analytical methods which do provide for frictional resistance. More importantly, these two analyses are not able to account for the experimental results for the 125 mm specimens, the majority of which failed by fibre fracture rather than pull-out.

The theories proposed by Lawrence [13] and Bartos [7] are fundamentally similar, as are the corresponding treatments of the experimental results, and hence the values of both maximum and "frictional" interfacial bond shear strength obtained using these theories are expected to be approximately equal. The differences are due to the inclusion of the test results for the 125 mm specimens in the calculation of the slope and intercept values describing the linear relationship

TABLE III Summary of estimated interfacial bond strength values

Analytical method	$\tau_{ib,max}$ (MPa)	$\tau_{ib,f}$ (MPa)	Comments
Greszczuk [3]	3.3		frictional resistance to slipping after adhesive bond failure not taken into account in analysis
Lawrence [13]	45.0	1.3	
Takaku and Arridge [4]	3.1		frictional resistance to slipping after adhesive bond failure not taken into account in analysis
Bartos [7]	38.4	1.2	
Laws [8]	94.7	1.2	calculated from test results for a very small number of specimens

between maximum pull-out load and embedded fibre length in the analysis using Lawrence's method but not Bartos'.

The highest value of maximum bond shear strength, i.e. approximately 95 MPa, is obtained by application of Laws' [8] extension of Lawrence's theory to a small number of test results of the appropriate form. Laws' description of the relationship between the debonding process and the pull-out load–fibre displacement curve seems to be the most sound of those proposed and hence the analysis based thereon should provide the most accurate estimate of the interfacial bond shear strength values. Unfortunately, however, it is not possible to assess the start of debonding, and hence estimate the $\tau_{ib,max}$ value, for specimens where the P_f–δ_f curve does not show a change in slope before the maximum load point is reached. The lack of such an obvious "debond" point in the majority of the pull-out curves obtained in this set of tests, i.e. those represented in Fig. 2b, may have been a result of the rapid progression of debonding along the fibre, and hence initiation of pull-out, due to the relatively low value of the "frictional" bond strength, $\tau_{ib,f}$.

It is difficult to compare the estimated values of interfacial bond properties obtained in the analyses described herein with those previously calculated for similar fibre–matrix combinations, as small differences in fibre surface condition, matrix composition, specimen curing conditions, and testing configuration can markedly affect pull-out test results [10]. It is interesting, however, that apparently significant differences are found in the estimated values of two parameters – the maximum interfacial bond strength ($\tau_{ib,max}$) and the coefficient of friction (μ) between the fibre and the matrix. The value of $\tau_{ib,max}$ calculated using Laws' method of analysis in particular is more than one order of magnitude larger than the value obtained by Laws herself from pull-out test results for a steel wire in a cement paste matrix [8], and the value of μ obtained from the "apparent" pull-out loads using the analytical method described by Takaku and Arridge [4] is about one order of magnitude smaller than that calculated by Beaumont and Aleszka [2] from pull-out test results for a steel fibre–cementitious mortar matrix using the same method. These findings suggest that, for this fibre–matrix combination at least, the relative influence of the adhesional bond strength on the maximum pull-out load is larger, whereas that of the frictional resistance to slipping is smaller, than had previously been shown theoretically [16].

The true values of the adhesional or elastic bond strength and the frictional resistance to slipping are not known and at best the values reported in Table III are reasonable estimates. In fact, in view of the variable and discontinuous nature of the interfacial bond at the microstructural level, these values may represent only the actual average adhesional bond strength along the interface, as opposed to the apparent average bond strength which is evidently dependent upon the embedded length of fibre in the test specimen (see Fig. 3), the true bond strength over localized areas certainly being substantially higher [17]. Nonetheless, it is the value of this actual average adhesional bond strength, together with that representing the frictional resistance to slipping, that is of practical importance in assessing the effect of various factors on fibre/matrix interfacial bonding and of this bonding on the mechanical properties of a composite material.

6. Conclusions

Analysis of the experimental test results for single fibre pull-out specimens with different embedded fibre lengths, consisting of a brass-coated steel wire fibre in a cementitious mortar matrix, using the relevant theories reviewed in the first part of this paper, leads to the following conclusions:

(a) For this fibre/matrix combination, the total resistance to interfacial debonding apparently consists of both adhesional bonding and, at sufficiently long fibre embedment lengths, frictional resistance to slipping after the adhesive bond has failed. The results indicate that there is no frictional resistance to slipping at fibre embedment lengths less than 2 to 3 mm, and that the relationship between maximum pull-out load and embedded fibre length is nonlinear in this region. For fibre embedment lengths greater than 2 to 3 mm, the maximum pull-out load–embedded fibre length relationship is linear, with the slope of the regression line being a function of the frictional resistance to slipping at the interface ($\tau_{ib,f}$).

(b) The theories which do not consider the contribution of the frictional resistance to slipping over a debonded portion of the interface in assessing the total resistance to fibre debonding and pull-out, those proposed by Greszczuk [3] and Takaku and Arridge [4], are not able to account

for those specimens which failed by fibre fracture rather than pull-out, although they do give values for the adhesional interfacial bond strength ($\tau_{ib,max}$) which seem to be reasonable.

(c) The theoretical explanation of the debonding process and the variation of maximum pull-out load with embedded fibre length, and the method of treating the experimental data to obtain estimated values for the mechanical properties of the interfacial bond, proposed by Lawrence [13] and Bartos [7] are essentially the same. There is no significant difference between the values of either the adhesional or the "frictional" interfacial bond strength obtained using these two methods.

(d) The theory proposed by Laws [8] seems to best describe the debonding and pull-out behaviour of steel fibre–cementitious matrix specimens. However, sufficient information was not provided by the pull-out load–time curves, particularly with regard to the load at which debonding starts, for enough of the specimens tested to enable proper assessment of this method of analysis.

Acknowledgements

The experimental work reported in this paper was carried out whilst the author was a graduate student in the Department of Civil Engineering at The University of Calgary. The financial support provided by the Natural Sciences and Engineering Research Council of Canada and The University of Calgary is acknowledged. The author is grateful to Professor C. D. Johnston for his advice and encouragement then and now.

References

1. R. J. GRAY, *J. Mater. Sci.* **19** (1984) 000.
2. P. W. R. BEAUMONT and J. C. ALESZKA, *ibid* **13** (1978) 1749.
3. L. B. GRESZCZUK, ASTM STP 452 (American Society for Testing and Materials, Philadelphia, 1969) p. 42.
4. A. TAKAKU and R. G. C. ARRIDGE, *J. Phys. D: Appl. Phys.* **6** (1973) 2038.
5. J. BOWLING and G. W. GROVES, *J. Mater. Sci.* **14** (1979) 431.
6. P. BARTOS, in Proceedings of the International Conference on Bond in Concrete, Paisley College of Technology, June 1982, edited by P. Bartos (Applied Science Publishers, London, 1982) p. 60.
7. P. BARTOS, *J. Mater. Sci.* **15** (1980) 3122.
8. V. LAWS, *Composites* **13** (1982) 145.
9. R. C. DeVEKEY and A. J. MAJUMDAR, *Mag. Concrete Res.* **20** (1968) 229.
10. R. J. GRAY, PhD Thesis, The University of Calgary, Calgary, Alberta, Canada (1982).
11. R. J. GRAY and C. D. JOHNSTON, in Proceedings of the RILEM Symposium on Testing and Test Methods of Fibre Cement Composites, The University of Sheffield, April 1978, edited by R. N. Swamy (The Construction Press, Lancaster, 1978) p. 317.
12. R. J. GRAY, in Proceedings of the International Conference on Testing, Evaluation and Quality Control of Composites, The University of Surrey, Guildford, September 1983, edited by T. Feest (Butterworth Scientific Ltd, 1983) p. 3.
13. P. LAWRENCE, *J. Mater. Sci.* 7 (1972) 1.
14. D. J. PINCHIN and D. TABOR, *Cem. Concr. Res.* 8 (1978) 139.
15. *Idem, J. Mater. Sci.* **13** (1978) 1261.
16. V. LAWS, P. LAWRENCE and R. W. NURSE, *J. Phys. D: Appl. Phys.* **6** (1973) 523.
17. D. TABOR, in Proceedings of the NATO Conference on Adhesion Problems in the Recycling of Concrete, Saint-Remy-les-Chevreuse, November 1980, edited by P. C. Kreijger (Plenum Press, New York, 1981) p. 63.
18. M. ANSON and K. NEWMAN, *Mag. Concr. Res.* **18** (1966) 115.

Received 7 April
and accepted 19 September 1983